Article

Effects of Atom Search-Optimized Thornthwaite Potential Evapotranspiration on Root and Shoot Systems in Controlled *Carica papaya* Cultivation

Ronnie Concepcion II [1,2,3,*], Jonah Jahara Baun [2,4], Adrian Genevie Janairo [1,2] and Argel Bandala [2,4]

1   Department of Manufacturing Engineering and Management, De La Salle University, Manila 1004, Philippines; adrian_janairo@dlsu.edu.ph
2   Center for Engineering and Sustainability Development Research—Intelligent Systems Research Unit, De La Salle University, Manila 1004, Philippines; jonah_baun@dlsu.edu.ph (J.J.B.); argel.bandala@dlsu.edu.ph (A.B.)
3   Center for Natural Sciences and Environmental Research—Soil and Plant Health Research Unit, De La Salle University, Manila 1004, Philippines
4   Department of Electronics and Computer Engineering, De La Salle University, Manila 1004, Philippines
*   Correspondence: ronnie.concepcion@dlsu.edu.ph; Tel.: +63-916-491-2138

Abstract: Potential evapotranspiration (PET) indicates if a cultivation area is suitable for planting. Currently, site-specific PET models that are based on large geographic regions are vulnerable to inaccurate predictions as a result of climate change and sudden changes in the environmental abiotic stressors that affect plant growth. For the aim of promoting the papaya Sinta F1 cultivar, the study optimized the standard Thornthwaite PET model by integrating three advanced physics-based metaheuristics and evolutionary computing, namely atom search (ASO), differential evolution (DE), and multiverse (MVO) optimizers. The PET value was optimized through minimization as a function of air temperature, light intensity, heat index, and extended heat index. As the PET value approaches 0, it indicates that there is more soil-water content that can be absorbed by plants. Based on the four cultivation treatments (uncontrolled, ASO, DE, and MVO) exposed in three replicates within 90 days, the ASO-optimized Thornthwaite PET-treated (ASO$_{Th}$) papaya plants resulted in the highest chlorophyll a and b concentrations, densest stomatal density, concentrated root and stem xylem and phloem vessels, considerable root and stem length, most formed leaf count, and strongest action potentials coming from stem membrane for both light and dark periods. This proves the applicability of the intelligent process in modifying the Thornthwaite model for plant growth promotion. Also, through the developed ASO$_{Th}$, the stem length and thickness ratio was improved for mechanical stability to facilitate more branching leaves and potential fruits during the fruiting stage, and the chlorophyll a and b ratio was enhanced, which naturally extended the light energy band for photosynthesis. Overall, the newly developed ASO$_{Th}$ model may be used to grow papaya seedlings year-round anywhere on Earth if there is a control system to regulate the environmental setting inside the growth chamber.

Keywords: atom search; controlled environment agriculture; differential evolution; multiverse optimization; plant electrophysiology; evapotranspiration; papaya cultivation

1. Introduction

Temperature erratically changes due to global warming and manifests cascaded disturbances to the natural and expected growth of crops and fruit-bearing trees worldwide [1]. In tropical and subtropical countries, papaya (*Carica papaya*) is a significant economic crop because of its large yield, practical qualities, nutritional values, and year-round fruit production [2,3]. It is known as a semi-woody, short-lived perennial herb that typically has a single stem and produces latex [3]. The photosynthetic process and growth of this

species can be influenced by edaphic and environmental factors such as wind, soil chemical and physical properties, light, relative humidity, air temperature, soil water content, and mineral nutrients, while production is affected by biotic variables like mycorrhizal fungus and genotype [4]. Moreover, water availability and sufficient tissue turgidity are required to preserve the stem's rigidity and boost productivity [3]. In real-world settings, papaya growers face several environmental issues made worse by climate change, which causes a negative growth impact and decreased profits [5]. The stages of growth of papaya fruit are affected by abnormal changes in weather due to climate change that result in delayed maturity, low quality of fruit, prolonged ripening, fruit sunburn, bad panicle emergence, poor color growth, and improper pollination [5]. Thus, global climate change is projected to have a great impact on agricultural growth, quality, and harvest [6,7]. It is critical to understand how climate change affects various aspects of crops, such as growth factors, crop water needs, and fruit output [6,7].

Recurring, unpredictable weather patterns influence the water balance of the soil, which alters evaporation and plant transpiration [8]. Evapotranspiration (ET) is known to be the water consumed by plants over a period and is frequently linked to rising temperatures, which could pose a major difficulty in fruit crop production of papaya [9]. The period's rising crop ET values have a significant effect on runoff and water supply [10]. Moreover, a drained soil water reservoir could result from higher evapotranspiration indices, which would cause water stress in plants during dry seasons [11]. As drought conditions are anticipated to grow more frequently, it will be crucial to protect the crop's productivity to understand how water constraints affect papaya physiology, particularly the photosynthetic processes [6]. The rising temperature affects photosynthesis immediately, causing changes in organic acids, contents of flavonoids, sugars, antioxidant activity, and firmness of crops [11]. The morphological and biochemical changes caused by exposure to high temperatures can have an impact on plant tissues and organ growth [11]. While both high temperatures and high moisture levels in papaya will result in increased total soluble solids (TSS), high temperature and high evapotranspiration make papaya trees lose their flowers, have a sudden change in sex, and also affect sterility [12]. The primary challenge in cultivating papaya seedlings is the poor microclimate along with abiotic elements that limit the ability to raise off-season fruit nurseries in dry regions [13]. Morphological parameters of papaya, including maximum germination, collar diameter, seedling height, shoot diameter, and the number of leaves, are substantially affected by temperature variations [13]. With these, potential evapotranspiration (PET) models such as the Thornthwaite, Penman–Monteith, Hargreaves, Blaney–Criddle, and Priestley–Taylor equations were formulated to provide a hypothetical reference for evaporation and transpiration under idealized conditions. However, the Thornthwaite PET might lead to inaccurate ET estimations for regions with extreme conditions and irradiation exposure [14]. The Penman–Monteith PET is data-intensive, and may not be available for all target regions [14]. The Hargreaves PET and Priestley–Taylor PET are simplified Penman–Monteith PETs but tend to be inaccurate for slow wind speeds and high humidity locations [15,16]. The Blaney–Criddle PET is crop-specific and requires crop coefficient parameters [17]. Due to these limitations and challenges with selecting a PET for specific crop cultivation and areas of interest, it is vital to modify and remodel existing PET models because doing so would be beneficial for both open agriculture and controlled environment agriculture (CEA).

PET models have been used in remote sensing and applied for irrigated agriculture, which has opened the use of soft computing applications to analyze and estimate evapotranspiration for different crops [18]. As big data become prevalent in agriculture, various AI algorithms such as fuzzy-genetic and regularization random forest, adaptive neuro-fuzzy methodology, convolutional neural network, wavelet conjunction heuristic, and multivariate adaptive regression splines (MARS) have been applied to estimate future crop evapotranspiration in a time series analysis. A study was conducted in Egypt to predict wheat crop evapotranspiration based on the Hargreaves technique using a deep neural network (DNN), with temperature and solar radiation as input data [19]. The

training and validation dataset covered the years 1970 through 2017, and the testing and prediction dataset covered the years up to 2035, yielding a monthly actual and predicted correlation of above 0.93. According to future climatic data, two regions would have an increase in crop evapotranspiration while the remaining area would experience a decrease, which depends greatly on the location's weather and environment [19]. In the different areas of East Malaysia with oil palm plantations, Iran with wheat fields, and China's spring maize croplands, the FAO-Penman–Monteith method was used to estimate plant actual evapotranspiration (ET). This series of experiments resulted in obtaining the best ET prediction models of the extreme learning machine algorithm tuned with the whale optimization algorithm (WOA-ELM), where the different environments affected the similarity of the results [20], the surface energy balance algorithm for land (SEBAL), where irrigation management avoids providing excessive water that could cause landslides while ensuring adequate cultivation [18], and the sparrow search algorithm integrated with ELM (SSA-ELM), which considered crop factors only [21]. Sensors were utilized in a Brazilian greenhouse to gather daily meteorological data, and lysimeter mass data were used to calculate crop evapotranspiration. To calculate crop ET, a 4-21-1 artificial neural network (ANN) architecture based on air temperature, relative air humidity, global sun radiation, and wind speed was established [22]. Since the model's performance had an R2 of 0.91 and MSE of 0.005, it was found that this strategy worked well in a protected environment. However, crop growth parameters were not considered to enhance ET [22]. Most existing studies agree that machine learning algorithms are accurate in predicting crop ET in either outdoor land areas [22–25] or in a protected environment [22,26]. But, in the essence of crop cultivation, effects on crops were neglected since optimizations are focused on estimating ET and not on its benefits on plant growth parameters and yield. This is also important because evapotranspiration is unique for different plants and growth stages [19,21].

To provide a protected environment for crop-growing, greenhouses are typically used through controlled environment agriculture (CEA), which emerged with the use of technology. Methods like vertical farming, rooftop gardens, large-scale crop production from factories, and equipment like LED lighting and water pumps enabling indoor planting and automation are now common in urban settings. Monitoring systems with the use of sensors in measuring parameters affecting cultivation produce time series data that can be collected offline or through cloud storage for remote accessing, wireless sensor networks (WSN), or IoT-based systems. This has made humans more knowledgeable on managing greenhouse systems to maximize crop yields using artificial intelligence [27]. ANN and intelligent machine vision were applied to LED control for precision lighting in indoor gardens where light intensity and spectrum were adjusted based on plant growth and needs [28]. In a vertical farming set-up, convolutional neural network (CNN) image processing models were applied to detect lettuce diseases as part of a pest control system. The machine learning model was trained with different pictures of lettuce diseases using ResNet50 and ImageNet [29]. Using AI for controls like deep neural networks, CNN, recurrent neural networks, Bayesian reinforcement learning, and deep deterministic policy gradient combined with a generative adversarial network, five global teams competed in a remote greenhouse-growing cucumber challenge in 2019. Cucumber production was significantly improved by AI-managed crop production systems with higher light intensity and a balanced CO_2 and ventilation environment [30]. ANN was also used to discover an effective drip irrigation technique for growing cucumbers in protected soil, obtaining higher yields [31].

Despite the large collections of formulated potential evapotranspiration models for various crops worldwide, there are still instances where it cannot be localized, especially with the additional influence of climate change and anthropological activities. Another factor for selecting an evapotranspiration model is the basis of predictors or natural factors that could affect it. It appears that based on the surveyed literature, the majority used models that have large arrays of parameters and are sometimes hard to measure by low-income and small-scale farmers [18–22,32]. Though those models are quite responsive, the

applicability of using them by general farmers is constrained. Issues like this can be solved by computational intelligence, particularly advanced physics-based metaheuristics and evolutionary computing for optimization purposes.

To address the challenge of an ineffective evapotranspiration model, this study optimized the Thornthwaite evapotranspiration model using atom search (ASO), differential evolution (DE), and multiverse (MVO) metaheuristics and applied the recommended best temperature in a controlled growth chamber for papaya seedling cultivation. ASO, DE, and MVO were the preferred computational intelligence algorithms as they did not result in premature convergence during the initial experiment and had fewer hyperparameters that could be easily reconfigured, unlike some recently developed optimization models [33–35]. Here, these three optimization algorithms were tested to explore the feasibility of the best solutions they provided in a realistic application for cultivation. Thornthwaite was the chosen potential evapotranspiration model because it has not been used yet as a basis for papaya cultivation, and it has a comparably limited number of factors to consider, unlike other more complex schemes such as the Penman [36] and Penman–Monteith models [14,37]. Given the simplicity of the Thornthwaite potential evapotranspiration model, if not customized to the requirement of a specific crop or fruit-bearing tree, it might negatively affect its photosynthesis and nutrient absorption, which is relevant to its growth and yield.

This study made the following contributions:

- Modification and optimization of the general Thornthwaite evapotranspiration model using physics-based (ASO and MVO) and evolutionary-based optimization (DE) concepts to make it site-specific and crop-specific. This resulted in a fitness function resembling PET_{Th-mod} with average monthly possible sunshine hour, mean temperature, heat index, and extended heat index as the exogenous variables. Optimizing the Thornthwaite PET configuration has the potential to induce crop growth and sustainability in precision farming.

- Elucidation of electrophysiological signals from papaya stem as affected by environment temperature, which was confirmed to be the most sensitive when the ASO-based Thornthwaite PET-controlled environment parameters were physically configured. This action potential coming from the papaya stem membrane serves as an indication of its sensitivity to external stressors.

- Comparison of resulting papaya leaf structure and chlorophyll, and root and stem vascular vessels and external architecture as influenced by temperature inside a controlled environment preset by ASO, DE, and MVO. This would substantiate the generated global best combinations of environmental parameters by advanced physics-based metaheuristics and evolutionary computing models integrated with Thornthwaite PET.

- Establishing a temperature-controlled environment agriculture for the Sinta F1 papaya genotype by inducing its natural vegetative seedling growth for year-round production.

2. Materials and Methods

This study is a biology experiment integrated with applied artificial intelligence. Five developmental stages were investigated, namely (1) initial papaya cultivation and pre-harvest growth factors acquisition, (2) Thornthwaite evapotranspiration optimization, (3) papaya electrophysiological signal extraction, (4) cultivation using the optimized evapotranspiration influencing factors based on computational intelligence, and (5) plant architecture and microscopy analysis (Figure 1). The goal of this study was to highlight the potential of computational intelligence in improving controlled-environment agriculture. MATLAB R2021b was the only computational intelligence software used in the study.
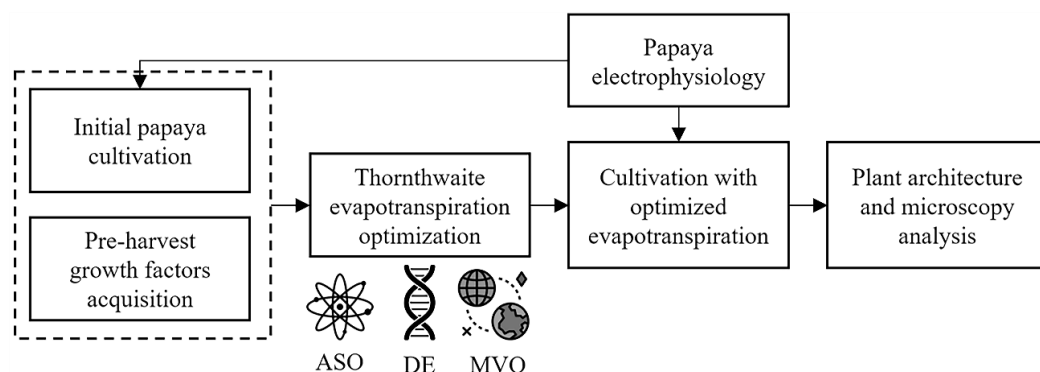
Figure 1. Developmental framework for the optimization of Thornthwaite evapotranspiration using atom search, differential evolution, and multiverse metaheuristics with electrophysiology for controlled papaya cultivation.

2.1. Plant Material and Cultivation Condition

Sinta F1 papaya (*Carica papaya*) from East–West Seed, Philippines, was the selected fruit-bearing tree genotype for this experiment as it is hard to cultivate this specific tree in Cavite, Philippines (experiment location: 14°27′26.676″ N, 120°55′42.4812″ E shown in Figure 2) due to combined heat extremes and high salinity in the soil system all year round. The study was focused on the vegetative plant stage (seedling) only, which lasts until the third month (90 days) of the growth cycle. Ten papaya seeds were germinated individually in 2.5 in × 6 in plastic containers with a soil composition of 40% loam, 30% sand, 10% perlite, and 20% vermiculite. This initial cultivation was performed in an uncontrolled open environment (Figure 2b,c) while measuring the temperature using a DS18B20 temperature sensor and Arduino ESP32 microcontroller (e-Gizmo Mechatronix Central, Philippines) that directly logs data to ThingSpeak IoT cloud storage every 30 min. Each pot was fertigated with 25%, 75%, and 100% strength of the formulated nutrient solution for the days after germination (DAG) 1-30, DAG 31-60, and DAG 61-90, respectively. The full strength nutrient solution was composed of 16 mM KNO_3, 6 mM $Ca(NO_3)_2 \cdot 10H_2O$, 2 mM $NH_3H_2PO_4$, 1 mM $MgSO_4 \cdot 7H_2O$, 50 µM KCl, 25 µM H_3BO_3, 2 µM $MnSO_4 \cdot H_2O$, 1 µM $ZnSO_4 \cdot 7H_2O$, 0.5 µM $CuSO_4 \cdot 5H_2O$, 0.5 µM $(NH_4)_6Mo_7O_{24}$, and 50 µM Fe-EDTA.
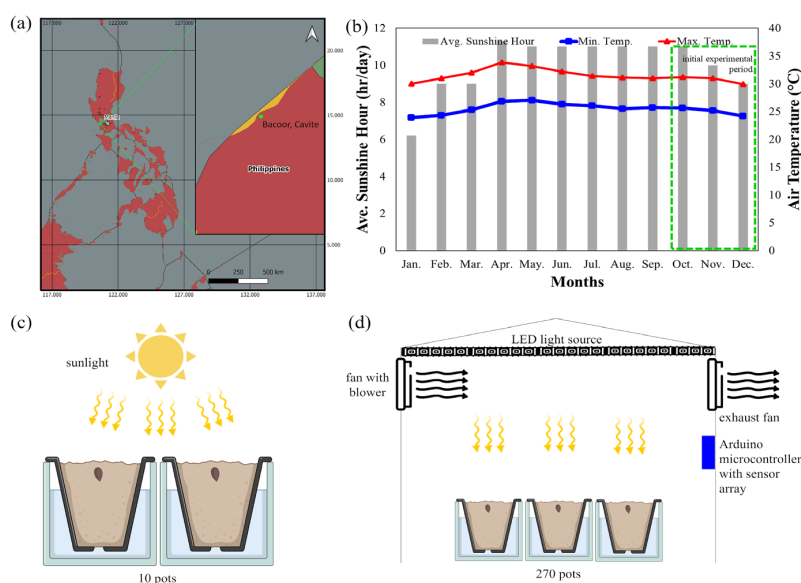

Figure 2. (**a**) Experimental location in the Cavite province of the Philippines, (**b**) environment temperature and average sunshine hours for the whole year of 2022 indicating the initial experiment, and the diagrammatic representations of (**c**) initial outdoor experiment setup and (**d**) controlled environment after the conduct of Thornthwaite PET optimization through computational intelligence approach.

2.2. Thornthwaite Evapotranspiration Optimization Using Advanced Metaheuristics

Thornthwaite potential evapotranspiration (PET_{Th}) is a referential measure characterized by the mathematical relationships of environmental parameters such as the average monthly possible sunshine hour (N, h/day), number of days of each month (m, days), mean temperature (T_m, °C), heat index (I, unitless), and extended heat index ($α$, unitless) (1–3). Here, N, m, T_m, I, and $α$ were set to minimum and maximum threshold pairs of [6.2 to 11.3 h/day], [29 to 31 days/month], [25.483 to 32.483 °C], [12.8 to 15.3], and [−6.9 to −4.3] based on initial acquired experimented data of the Philippines from 2019 to 2021 [38–40]. The goal of this stage was to optimize the modified PET_{Th} (PET_{Th-mod}) as a function of {N, T_m, I, $α$} (4), serving as the fitness function, through minimization using atom search (ASO), differential evolution (DE), and multiverse optimization (MVO) to reduce plant stress due to drought when there is substantial high temperature (Figure 3).

$$PET_{Th} = 16(\frac{N}{12})(\frac{m}{30})(\frac{T_m}{I})^{α}, \tag{1}$$

$$I = \sum_{i=1}^{12} (\frac{T(i)m}{5})^{1.514}, \tag{2}$$

$$α = 6.75 \times 10^{-10} I^3 - 7.71 \times 10^{-5} I^2 + 1.79 \times 10^{-2} I + 0.49, \tag{3}$$

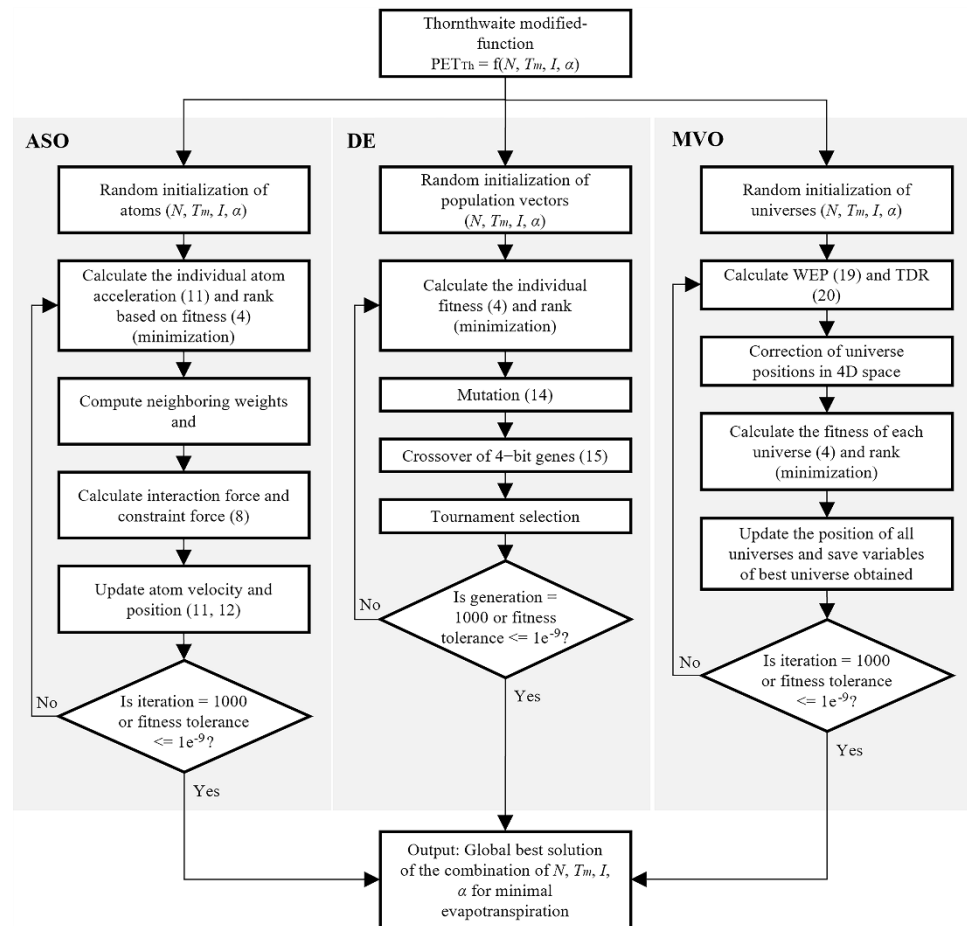$$PET_{Th-mod} = 1.356N(\frac{T_m}{I})^{α}. \tag{4}$$

Figure 3. Optimization framework for Thornthwaite evapotranspiration model using atom search, differential evolution, and multiverse optimization algorithm.

ASO is a recently developed population-based heuristic algorithm that draws inspiration from physics and imitates the atomic motion governed by interaction and constraint forces to create an efficient search mechanism for large-scale optimization issues [33,41]. In ASO, each atom in the initial iteration interacts with the others through repulsion and attraction, and repulsion can prevent an excessive concentration of atoms and an early convergence of the algorithm, improving the ability to explore the whole search space [33,41]. The attraction steadily grows stronger, and the repulsion gradually recedes as iterations go by, signaling that the exploration is decreasing and the exploitation is escalating [33]. Each atom in the final iterations interacts with the others simply through attraction, ensuring that the algorithm has a good capacity for exploitation. Equation (5) describes the overall interaction forces acting on the ith atom in the dth dimension and the vector sum of the repulsion and attraction that the ith atom experiences from dynamically shifting neighbor atoms where *Kopt* is a subgroup of the population of the atom that consists of initial K atoms with the optimum values of fitness function and $rand_j$ is a random number in the range of [0, 1]. The interaction force operating on the ith atom from the jth atom in the dth dimension at t time is denoted by the Lennard–Jones (L–J) potential in (6), where $h_{ij}(t)$ is the ratio of the distance between two atoms to the length scale $\eta(t)$ that is the depth function for altering the region's repulsion or attraction (7). $\eta(t)$ is affected by α as the weight of depth, while T is the maximum number of iterations. Here, if every single atom in the ASO has a covalent bond with the optimum atom, the normalized position weight difference between the atom and the optimum atom, known as geometric constraint force, can be expressed as (8) where $x_{opt}^d(t)$ is the position of the optimum atom in the dth dimension, and $\lambda(t)$ is the Lagrangian multiplier, where β is the weight of the multiplier (9). The acceleration of the ith atom in the dth dimension at iteration t can be calculated from the given interaction and constraint force arising from the bond-length potential and L–J potential as a function of $m_i(t)$ as the mass of the ith atom at the tth iteration, which can be determined by its fitness function value in (10). Finally, to make the algorithm simpler, the velocity (v) and the position (x) of the ith atom at $(t + 1)^{th}$ iteration can be expressed as (11) and (12).

$$F_i^d(t) = \sum_{j \in Kopt} rand_j F_{ij}^d(t), \tag{5}$$

$$F_{ij}^d = -\eta(t)\left[2\left(h_{ij}(t)\right)^{13} - \left(h_{ij}(t)\right)^7\right], \tag{6}$$

$$\eta(t) = \alpha\left(1 - \frac{t-1}{T}\right)^3 e^{-\frac{20t}{T}}, \tag{7}$$

$$G_i^d(t) = \lambda(t)\left(x_{opt}^d(t) - x_i^d(t)\right), \tag{8}$$

$$\lambda(t) = \beta e^{-\frac{20t}{T}}, \tag{9}$$

$$m_i(t) = \frac{M_i(t)}{\sum_{j=1}^N M_j(t)}, \tag{10}$$

$$v_i^d(t+1) = rand_i^d \cdot v_i^d(t) + a_i^d(t), \tag{11}$$

$$x_i^d(t+1) = x_i^d(t) + v_i^d(t+1). \tag{12}$$

DE is one of the straightforward evolutionary techniques that was found to have strong performance in global optimization [34]. Differential knowledge is primarily employed to direct its subsequent search, and the fundamental components of its optimization process are mutation, crossover, and selection, with mutation serving as the primary determinant of DE's optimization adaptability [42]. The DE method begins the investigation with a

population of potential solutions that are initialized at random in the entire search space using (13), where $rand_i^j(0,1)$ signifies an evenly distributed random number within the range of [0, 1], which is individually instantiated for each member. X_{min}^j and X_{max}^j are the lower and upper bounds on each decision variable, respectively [43]. In this study, following population initialization, DE applies the following strategies for mutation, crossover, and selection. In mutation, three different agents, X_{r1}, X_{r2}, and X_{r3}, are chosen from the current population to carry out the mutation operator, where $r_1 \neq r_2 \neq r_3 \neq i$ is used to produce a mutant vector U_i. The mutator can be represented mathematically as in (14), where F is the mutation scale factor, which is a vector of D dimensions. The scaling factor (*F*) performs as a positive control parameter to measure the vector difference. The notation "DE/a/b" denotes the DE mutation methods, where "a" stands for the base vector to be disturbed and "b" for the number of differential vectors [43]. After the mutation process, the trial vector V_i is produced by performing a crossover operation between the target vector X_i and the mutant vector U_i. DE uses either a binomial crossover or exponential crossover operation to create a trial vector. The crossover operator can be denoted as (15), where P_{CR} is a probability factor in defining the swarm diversity and inhibits the algorithm from shrinking into local minima, rand is a number randomly in the range [0, 1], and j_{rand} is an index number, arbitrarily produced between {1, 2, ..., D}. This guarantees that one component of the trial vector V_i happens to be from mutant vector U_i. The selection operator indicates that the trial vector V_i and the search agent X_i are evaluated or compared in terms of their fitness values, and the best offspring is selected. This can ensure that the best potential solution will be preserved, optimizing the algorithm's speed and accuracy of convergence [42].

$$X_i^j = X_{min}^j + rand_i^j(0,1) * \left(X_{max}^j - X_{max}^j\right), \tag{13}$$

$$U_i = X_{r1} + F \times (X_{r2} - X_{r3}), \tag{14}$$

$$V_{ij} = \begin{cases} U_{ij}; & rand(0,1) < P_{CR} \ or \ j == j_{rand} \\ X_{ij}; & otherwise. \end{cases} \tag{15}$$

The MVO algorithm is inspired by the concept of multiverse theory, where the white hole and black hole can interact through a wormhole as a travel path [35,44]. This algorithm takes the solution as a universe; therefore, the population size is the total number of universes. Inputs are the population size and the maximum number of iterations. The fitness of a solution is determined by the assigned inflation rate (IR), in which the best solution has the lowest value. The first stage of MVO is an exploration that aims to determine the most applicable regions in the search space that could contain the best local optima with white holes and black holes. The second stage, exploitation, makes use of wormholes to extract the local optima from the regions to determine the global optimum. MVO is guided by rules in determining the white holes and black holes and how the objects move through the wormhole: the higher the IR, the higher probability of having a white hole; the higher the IR, the lower probability of having a black hole; universes with higher IR tend to send objects through white holes; universes with lower IR tend to send objects through black holes; the objects in all universes will experience random movement towards the best universe via wormholes regardless of IR [35,44]. A population of the universe (*U*) is represented by a matrix (16) where d denotes the number of solution parameters or variables, and *n* is the total number of universes. The exchange of objects occurs during every iteration using the roulette wheel mechanism. The selection of a universe is based on (17), where x_i^j is the jth variable of the ith universe, x_k^j is the jth variable of the kth universe from roulette selection, and $r1$ is a random constant from 0 to 1. Here, the universe can exchange objects, assuming that a wormhole tunnel connects a universe to the best universe in a region to provide local exchange in each universe. These exchanges of objects between universes are represented by (18). The acronyms TDR and WEP are coefficients of the

traveling distance rate and wormhole existence probability, respectively. The variable X_j is the jth parameter, while the upper and lower bounds of the jth parameter are represented by ub_j and lb_j, respectively. Variables $r2$, $r3$, and $r4$ are any number between 0 and 1. The coefficient TDR defines the traveling speed of an object towards the best universe, while WEP defines the existence in the universe (19) and (20), where l is the current iteration, and L is the total number of iterations. The min and the max indicate the maximum and minimum values of r, and p is the exploration accuracy. TDR and WEP are updated and assigned to each universe during every iteration. After which, the process repeats, selecting a universe as a white hole among the sorted universes according to the updated IR and through roulette wheel selection. This will proceed again to exchange objects between different universes [44]. The iteration will end when the stopping criteria are matched, which could be the maximum number of iterations or the number of non-improvement iterations, which occurs when the best solution is not updated after n successive iterations.

$$U = \left[x_1^1 \, x_1^2 \, \cdots \, x_1^d \, x_2^1 \, x_2^2 \, \cdots \, x_2^d \vdots \ddots \vdots \, x_n^1 \, x_n^2 \, \cdots \, x_n^d \right], \tag{16}$$

$$U = \left\{ x_k^j \quad r1 < Normalized\ IR\ (Ui) x_i^j \quad r1 \geq Normalized\ IR\ (Ui), \tag{17} \right.$$

$$x_i^j = \left\{ \left\{ X_j + TDR \quad \times \left(\left(ub_j - lb_j \right) \times r4 + lb_j \right) \quad r3 \right. \right.$$
$$< 0.5 \qquad\qquad X_j + TDR \times \left(\left(ub_j - lb_j \right) \times r4 + lb_j \right) \quad r3 \tag{18}$$
$$< 0.5 \quad r2 < WEP \ x_i^j \qquad\qquad\qquad\qquad\qquad r2 \geq WEP,$$

$$WEP = +l \times \left(\frac{-min}{L} \right), \tag{19}$$

$$TDR = 1 - \frac{l^{1/p}}{L^{1/p}}. \tag{20}$$

Summarized in Table 1 are the hyperparameters configured in the finalized-converged form of ASO, DE, and MVO. The recommended global best solutions of ASO, DE, and MVO, the environment temperature suitable for reduced evapotranspiration, were individually set in a cultivation chamber for the analysis of the impact of temperature on papaya growth phenes. This is expected to correspond with a $PET_{Th\text{-}mod}$ value that is close to 0, which pertains to a very low rate of water evaporation in that enclosed environment. For the cultivation with an optimized evapotranspiration environment as recommended by ASO, DE, and MVO, 30 papaya seeds were tested for each treatment with three replicates totaling 270 seeds (30 seeds per treatment × 3 treatments × 3 replicates per treatment). Figure 2d shows the diagrammatic setup for this controlled environment experiment.

Table 1. Summary of hyperparameters configured using ASO, DE, and MVO.

Atom Search Optimizer	Differential Evolution	Multiverse Optimizer
No. of atoms: 150	Population size: 150	No. of universes: 150
Maximum iteration: 1000	Maximum generation: 1000	Maximum iteration: 1000
Inertia weight: 0.9	Mutation rate: 0.9	Expansion rate: 0.9
Acceleration coefficient: 0.8	Mutation strategy: Uniform	Contraction rate: 0.8
	Crossover rate: 0.8	Gravity coefficient: 0.9
	Selection rate: 0.9	No. of universes: 150
	Selection strategy: Tournament	

2.3. Papaya Electrophysiological Signal Extraction

Biosignals from the papaya stem in the form of a DC voltage signal were sampled every 30 min for 90 days. One electrode (red) was inserted through the vascular tissues of the papaya stem, 2 cm above the soil line, and another electrode connected from the ground terminal of the AD620 amplifier was directly buried 5 cm from the soil system and 3 cm distant from the papaya stem to complete a circuit (Figure 4). The electrodes were made of Ag-coated Cu-pin-type cylindrical metal with 0.05 mm^2 surface area. Because the voltage sensor and ESP32 Arduino microcontroller operate at 5 V, the minimum input voltage that this system can read is 24.25 mV (5 V)^2/1023-bit resolution). The average electricity that can be extracted from the papaya stem is 100 μV; hence, the configured gain for AD620 was set to 25 to ensure other lower voltage spikes were acquired. This electrophysiological experiment was performed in uncontrolled and controlled cultivations, thus verifying the variations in the stem signals due to differences in environmental temperature.
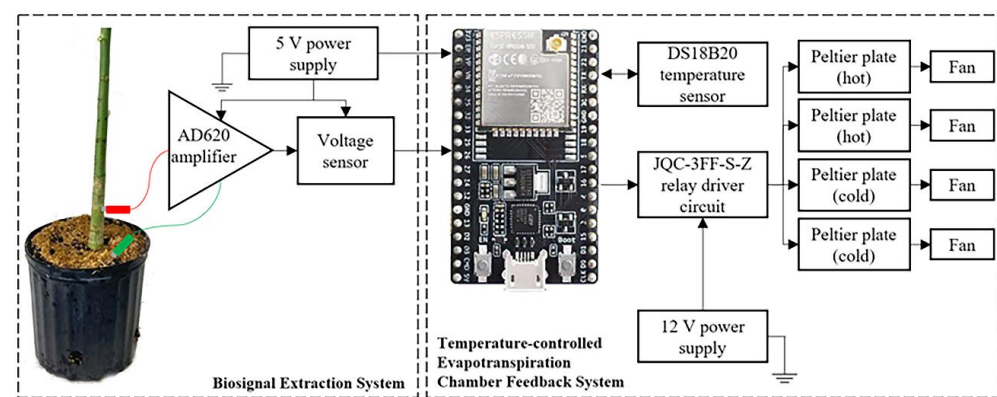

Figure 4. Setup for extracting biosignals from papaya stems (**left**) and electronic system block diagram for the controlled cultivation greenhouse as recommended by the integrated advanced metaheuristics (**right**).

2.4. Plant Phenotyping and Vascular Tissues Microscopy

Morphological phenotypes and anatomical vascular tissues were measured at the end of 90 DAG to clearly delineate the manifestation of uncontrolled temperature and ASO-, DE-, and MVO-optimized environmental temperature. Root and stem lengths were measured using a digital caliper. Leaf counts were counted manually. Chlorophyll-a (Chl-a, $C_{55}H_{72}MgN_4O$) and chlorophyll-b (Chl-b, $C_{55}H_{70}MgN_4O_6$) were measured by sampling 1 g of leaf tissue per treatment mixed with 75% acetone solution and submerged in a hot bath of 60 °C for 30 min. The solution was then passed through a filter paper, and absorbance was measured using a UV-Vis 1900 spectrophotometer at 663 nm and 470 nm for Chl-a and Chl-b, respectively [45,46]. Stem tissues 1 cm from the internode of hypocotyl and root system were sectioned transversely and stained with 10% toluidine blue solution for 30 s, then decanted to an 80% acetic acid solution for 10 s, and lastly, washed with deionized water until excess dyes were removed. The same cell staining process was performed for root tissues dissected transversely 1 cm below the internode connecting to the main stem. Leaf tissues were sampled from the abaxial middle portion of the leaf for stomata counting. Tissue samples were imaged using a compound light microscope with 4× to 40× magnification (Howel Microscopes, Whitesboro, NY, USA). Micrographs were analyzed using ImageJ software to determine xylem, phloem, and stomata density per mm^2.

2.5. Statistical Analysis

Experiment data were analyzed using Pearson's correlation coefficient ($p < 0.05$). Correlogram and principal component analysis (PCA) biplot generation were all conducted in Minitab 20.4. Plant phenotype data were subjected to ANOVA with Tukey's honestly significant difference (HSD) comparison test in Minitab 20.4 to elucidate the significant differences among the three replicates of cultivation of the four treatments, namely, uncontrolled and the ASO-, DE-, and MVO-based Thornthwaite PET environment configurations.

3. Results

3.1. Dynamic Relationships of Cultivation Temperature and Papaya Phenes

The growth of papaya was measured based on chlorophyll a and b concentrations, stomatal density, root xylem and phloem densities, stem's xylem and phloem diameters, and root and stem lengths (Figure 5). Based on the 90-day experiment cultivating the Sinta F1 papaya plant, stem phloem diameter was observed to have a very strong negative correlation ($R^2 = -0.93 \pm -0.035$, $p < 0.05$) with other plant morphological and pigment phenotypes in an uncontrolled environment with Thornthwaite potential evapotranspiration of 283.403×10^{-3} (Figure 5). This interesting finding implies that as the dicotyledonous plant matures with reference to elongating roots and stems, the phloem diameter of the stem decreases; hence, a type of natural nutrient distribution optimization is facilitated by the plant. This phenomenon was not observed in monocotyledonous plants, as the usual observation was that the whole vascular bundle increased in diameter while the whole plant grew. Another emerging issue here is that if the stem length continues to grow, the phloem vessel will continue to become thinner (Figure 5b). The high environmental temperature was previously confirmed to have a direct impact on deteriorating phloem [17]. This is where optimizing potential evapotranspiration is required.
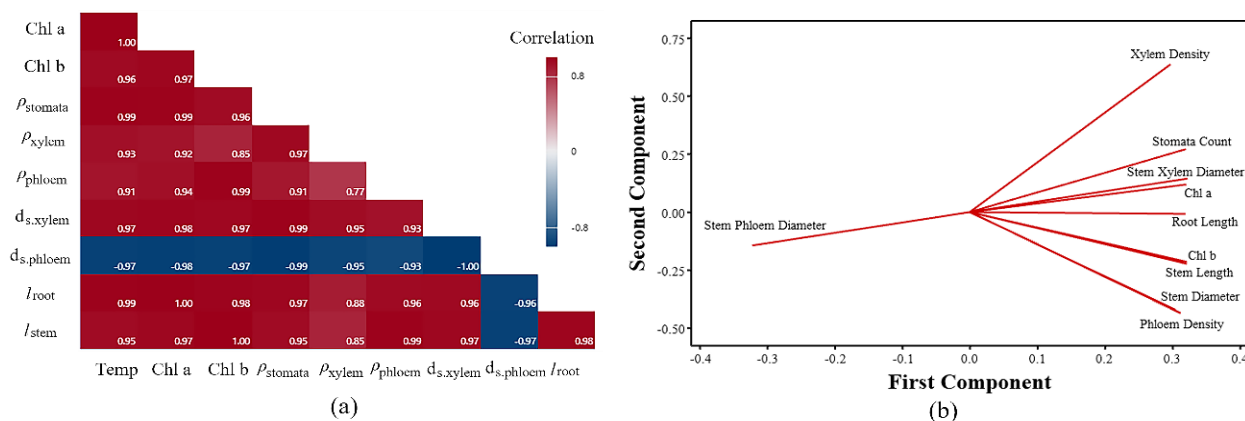

Figure 5. Dynamic relationships of cultivation temperature and papaya phenes through (**a**) a correlation map and (**b**) a principal component biplot.

3.2. Differential Impacts of ASO, DE, and MVO-Optimized Thornthwaite Evapotranspiration Model to Papaya Seedling Phenes and Anatomy

In total, 1000 iterations were used to explore and exploit the ASO, DE, and MVO algorithms in a 4D space to find the optimum combinations of the average monthly possible sunshine hour, mean temperature, heat index, and extended heat index to minimize the PET_{Th-mod}, ASO, DE, and MVO converged at iteration 845, 568, and 40, respectively (Figure 6). MVO exhibited premature convergence characterized by swift exploration that may result in unsearched 4D space. This was supported by a PET_{Th-mod} value of 23.723×10^{-3} (Table 2). On the other hand, the ASO and DE-optimized PET_{Th-mod} exhibited a more acceptable minimization trend (Figure 6) and a potential evapotranspiration value of 6.420×10^{-3} and 11.133×10^{-3} (Table 2). ASO-based PET_{Th-mod} (ASO_{Th}) was only a 0.271 factor of MVO_{Th}, and DE_{Th} was just 0.469. With this, ASO_{Th} was considered

to have the most recommended environment configuration (Table 2), especially concerning the mean temperature which was 31.664 °C and a heat index of 14.1 for a controlled environment setup. These findings for ASO_{Th} suggest that having a controlled system that would maintain a 10.033 h/day of sunshine hour, 31.664 °C mean temperature, 14.1 heat index, and -5.528 extended heat index would minimize the potential of evapotranspiration close to 0. The uncontrolled condition with a PET of 0.283 was not close to 0, but when compared to the ASO_{Th}, it was 44.146 times higher. Therefore, based on the integration of evolutionary computing in optimizing the environmental stressors, particularly the mean ambient temperature and light period, the ASO_{Th} configuration (Table 2) was considered the most recommended condition as it had the smallest rate for water-deficit vegetation. This specific ASO_{Th} configuration is recommended only for the Sinta F1 papaya variety and not for the general species.
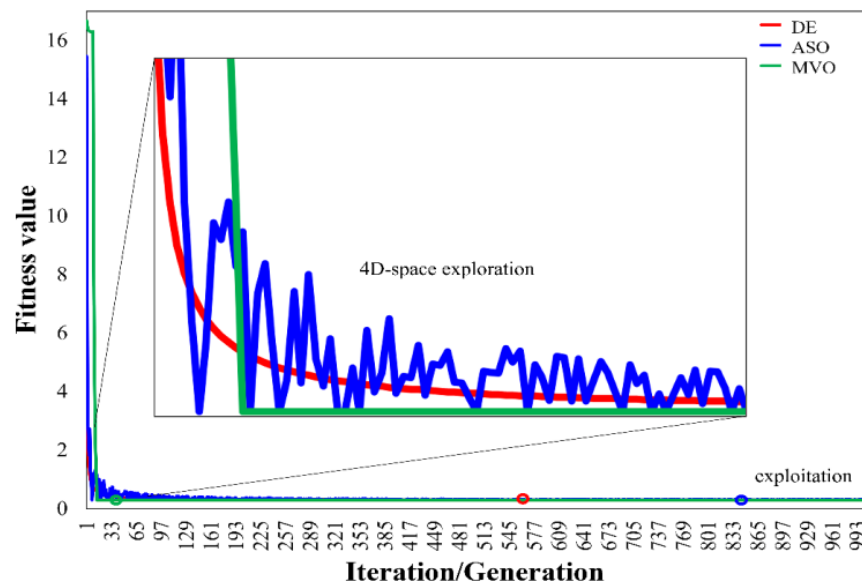

Figure 6. Fitness convergence of ASO, DE, and MVO to optimize the Thornthwaite potential evapotranspiration with respect to N, T_m, I, and α.

Table 2. Established recommended influencing parameters based on uncontrolled optimization algorithms to induce Sinta F1 papaya seedling growth.

Treatment/Model	Pre-Harvest Growth Parameters				PET_{Th}	$PET_{Th\text{-}mod}$
	N (h/day)	T_m (°C)	I	α		
Uncontrolled	10.042	28.483	13.900	-5.400	0.283	-
ASO_{Th}	10.033	31.664	14.100	-5.528	-	6.420×10^{-3}
DE_{Th}	12.100	30.532	15.500	-7.068	-	11.133×10^{-3}
MVO_{Th}	11.217	28.909	14.200	-5.718	-	23.723×10^{-3}

Based on modified Thornthwaite PET responses, the PET value approaches 0 when the minimum temperature is above 27 °C, the maximum temperature is between 31 °C and 33 °C, and the daily light period is 10–12 h (Figure 7a,b). In addition, with these configurations, the derivative Thornthwaite PET parameters, such as heat index and extended heat index, should be above 15 and below -6.5 (Figure 7c,d) to avoid excessive water loss in the soil system.
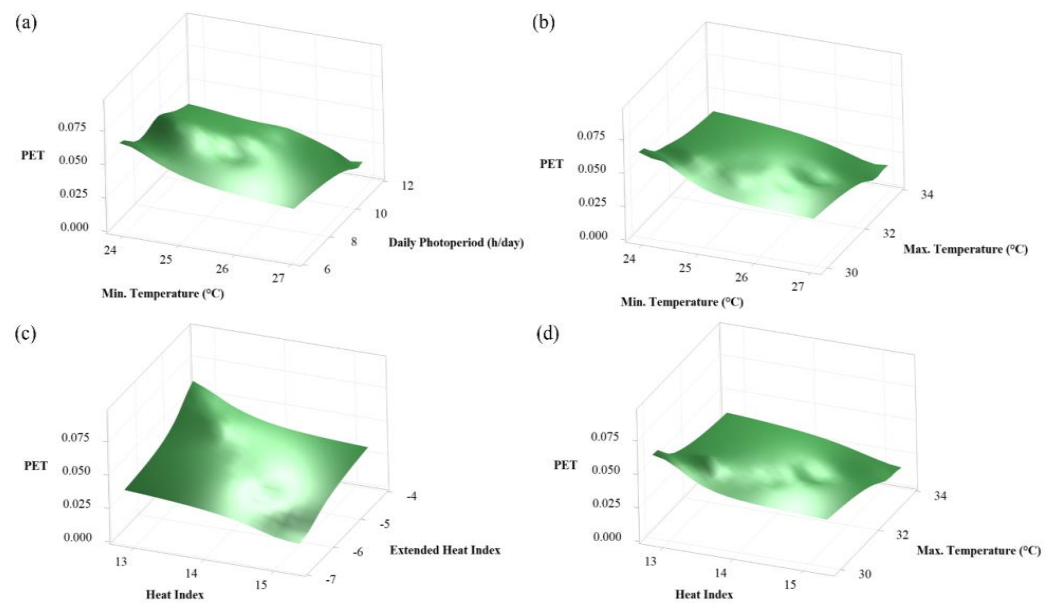
Figure 7. Three−dimensional surface graphs correlating the Thornthwaite PET for various impact combinations of (**a**) daily light period (N) and minimum temperature (T_{min}), (**b**) maximum temperature (T_{max}) and T_{min}, (**c**) I and α, and (**d**) I and T_{max}.

To verify the effectiveness of modified Thornthwaite PETs through ASO_{Th}, DE_{Th}, and MVO_{Th}, the plant's architectural and stem's vascular tissue were exposed and analyzed (Figure 8a,b). The chlorophyll *a* and *b* concentrations of ASO_{Th} were very strong at 2.843 mg/g and 0.877, respectively, with an average of 114 active stomata/mm^2 in the leaves (Figure 9a,b). In comparison with the stomata density of other treatments, the uncontrolled, DE_{Th}, and MVO_{Th} had factors of 0.509, 0.851, and 0.753 compared to that of the ASO_{Th}, respectively. This is logical as the chlorophyll *a* and *b* concentrations for uncontrolled, DE_{Th}, and MVO_{Th} treatments dropped by 267.419%, 715.3%, and 671.77%, respectively. Because the opening and closing of stomata are affected by the temperature and humidity of the environment, it is confirmative that the temperature recommended by ASO_{Th} is optimum for the Sinta F1 papaya cultivar. The 31.664 °C air activates the guard cells of stomata to open and allows the uptake of carbon dioxide and chlorophyll molecules to absorb light energy, promoting photosynthesis. The papaya seedling root exposed to ASO_{Th} treatment exhibited extended root system architecture (156.3 mm), 248.885%, 141.961%, and 215.586% longer than uncontrolled, DE_{Th}, and MVO_{Th} treatments, respectively (Figure 9c). The stem length of ASO_{Th} treatment exhibited extension to approximately 510.8 mm, 162.082%, 128.277%, and 140.407% longer than uncontrolled, DE_{Th}, and MVO_{Th} treatments, respectively (Figure 9c). Interestingly, the plant vegetative aspect ratio or the stem length and diameter ratio for the uncontrolled treatment resulted in 76.866, while the evolutionary-based treatments ASO, DE, and MVO resulted in 69.973, 75.132, and 64.964 (Figure 9d). As this vegetative aspect ratio passed the value of 100, the resembled plant stem was very thin [5,6]. This finding confirmed that ASO_{Th}-treated papaya plants have normal stem growth with improved mechanical stability. By having not too long and thin a stem, such as the uncontrolled treatment, the ASO_{Th}-treated plant had a reduced risk of breakage due to wind or mechanical stresses that might occur while it grows. Moreover, it was observed that the stem of ASO_{Th}-treated papaya exhibited the densest xylem (70 xylems/μm) and the sparsest phloem (33 xylems/μm) (Figure 9f,g). Despite the ASO_{Th} having a 10.033 h/day light period that was the least among the other treatments, including the uncontrolled, it exhibited the highest mean temperature of 31.664 °C. This caused the xylem vessel to be denser to help in water transport. Because of the advantageous environment in following the ASO treatment, there is no need for the papaya plants to develop denser phloem in transporting organic nutrients as by-products of photosynthesis

in growing leaves. It is noticeable that the uncontrolled treatment induced the plants to adjust to the environment by developing denser phloem to compensate for the temperature and other stressors in growing leaves (Figures 8a and 9f,g). In this study, the plants exposed to evolutionary computing-based Thornthwaite PET treatments were revealed to have a higher xylem–phloem ratio (Figure 9f,g), which suggests that the provision of minimal irrigation would still promote growth to the plants as they allocate more resources in xylem vessels responsible for water uptake. This is confirmed by the deeper root growth in ASO treatment (Figure 8a). Nonetheless, such an ASO-based cultivation chamber may have some benefits to the farmer for lesser water consumption while still producing an acceptable yield. Moreover, the chlorophyll a and b ratio, which is the ratio of pigments responsible for capturing light energy and the molecule that extends the range of absorbable light for photosynthesis, was higher in ASO_{Th}-treated papaya seedlings (approaching 4), and the uncontrolled treatment was up to the 1.5 level only (Figure 9h).
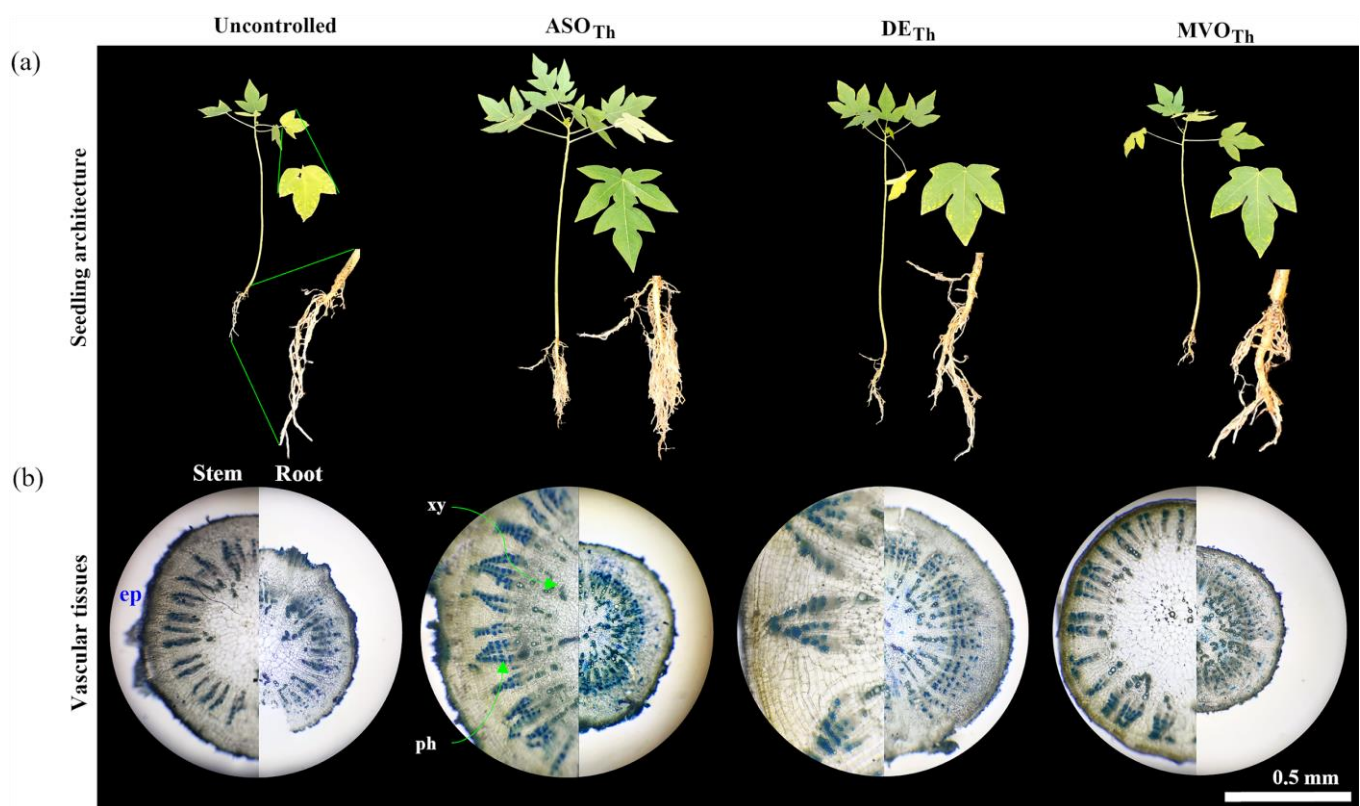

Figure 8. Impacts of cultivation temperature as observed in the (**a**) harvested papaya seedling architecture and (**b**) transverse sections of vascular tissues (stem and root) for each temperature treatment stained with TBO. (ep, xy, and ph mean epidermis, xylem, and phloem). Note that ASO_{Th}, DE_{Th}, and MVO_{Th} are the optimized Thornthwaite evapotranspiration model using ASO, DE, and MVO, respectively.
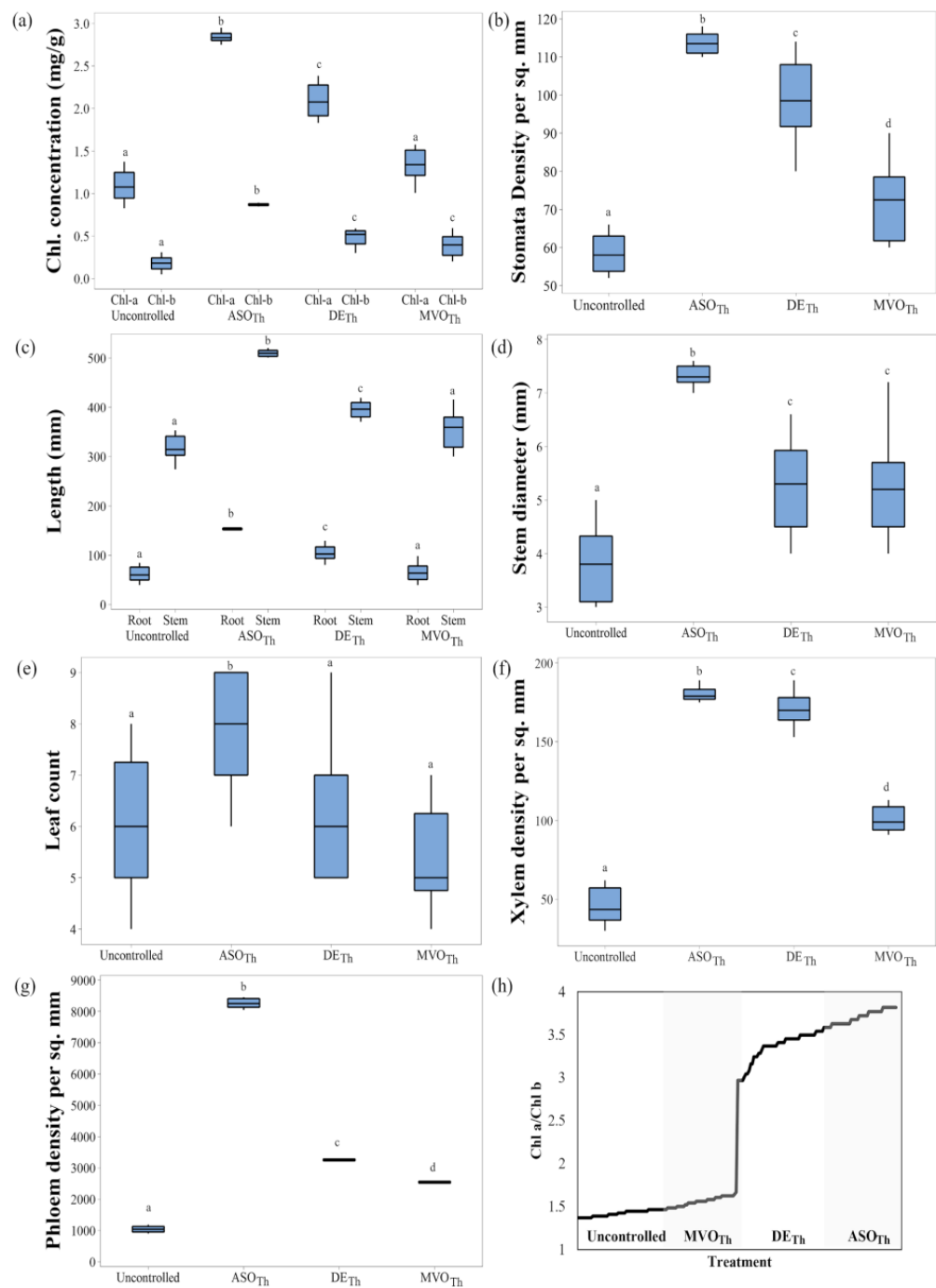
Figure 9. Measured (**a**) chlorophyll concentration, (**b**) stomata density, (**c**) root and stem lengths, (**d**) stem diameter, (**e**) leaf count, (**f**,**g**) xylem and phloem density, and (**h**) chlorophyll a and b ratio in relation to uncontrolled and modified Thornthwaite treatments. Note that ASO_{Th}, DE_{Th}, and MVO_{Th} are the optimized Thornthwaite evapotranspiration model using ASO, DE, and MVO, respectively. Groups a, b, c, and d within factors (treatments) with the same letter are not significantly different at 5% HSD.

3.3. Dynamics of Papaya Electrophysiological Signals

The action potentials or stem signals in papaya plant membranes were recorded using the Ag-coated Cu-pin type electrodes inserted across the vascular tissues (Figure 5), which resulted in a periodic oscillating signal waveform, as shown in Figure 10. It is remarkable that the ASO_{Th}-treated papaya plants exhibited the highest action potentials all day long throughout the cultivation period, that is, even during the dark period before

and after the scheduled light period (Figure 10). During the 10.042 h light period, the high action potentials incurred by the ASO_{Th} plants are an indication that stomata are open and active in performing the carbon dioxide and oxygen exchange [5]. In such cases, light photosynthesis happens with an average action potential of 200 mV across plant stems. During the light period, the uncontrolled treatment exhibited the weakest stem signal with an average value of 120 mV. This confirmed that the photosynthetic rate in the uncontrolled treatment is not the optimum condition for papaya plants. For a 1-day analysis, it is comparable that the action potentials from the stem have slightly higher readings in the dark period after the light period than before the light period (Figure 10). The probable cause of this is that the plant system is still slightly active processing due to residual energy induced during the light period. Here, it has been elucidated that action potential, chlorophyll *a* and *b* ratio, and stomata density have a positive relationship and, therefore, a considerable set of physiological parameters in understanding plant growth with respect to environment temperature and light period.
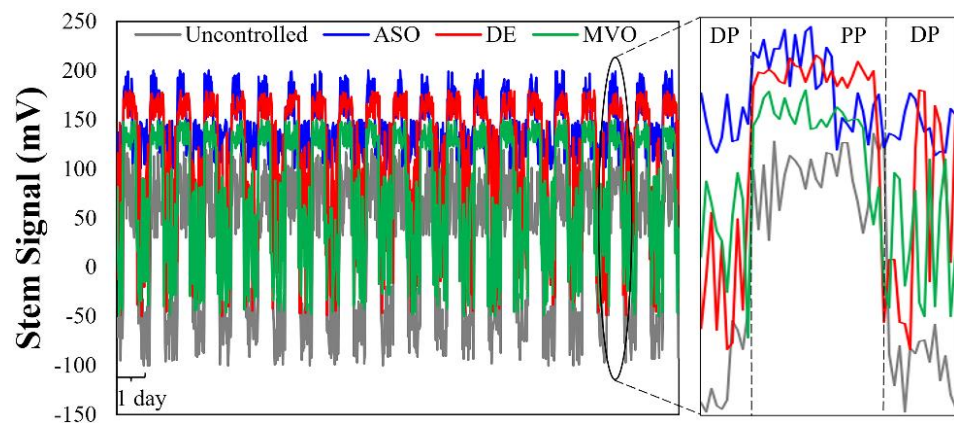

Figure 10. Recorded average stem signal from 10 papaya seedlings for each treatment with 100 Hz band filtering. DP and PP represent the dark period and the light period.

4. Discussion

Because of global warming and the effects of climate change, such as changes in rainfall patterns, the need to control certain environmental stressors would likely occur in order to improve crop productivity and yield. It was observed that a consistent pattern of irradiation improved the circadian rhythm of plants so they could optimally allocate their resources for growth and development [10,21]. In relation to the current study, the evolutionary computing models developed, namely, ASO, DE, and MVO, induced similar patterns of stem action potentials, showing a good indication of plants adapting to controlled environments. Thornthwaite potential evapotranspiration is a relatively simple indicator for water and thermal stressors in plants; together with other PET models like Penman–Monteith, Hargreaves, Priestley–Taylor, and Blaney–Criddle, it is used for geographical region-based analysis of sunshine hours, environment temperature, frequency of raining, and solar irradiation covering a wide region [14–17]. Hence, the selection of an applicable set of geographical parameters for evapotranspiration prediction and optimization has a strong impact on the potential agricultural productivity. The novelty of the current study is the development of an evolutionary-based Thornthwaite PET site-specific and crop-specific model (Figures 3 and 11). This model established that air temperature close to 31.5 °C and a light period between 10 to 10.5 h/day would optimally activate chlorophyll a and b molecules (Figure 11a,b), essentially activate most of the stomata in the adaxial surface of papaya leaves (Figure 11c), develop a denser xylem and phloem root and stem system (Figure 11d,g), induce both primary and secondary growth of the root and stem (Figure 11i,j), and strengthen the action potential from the stem membrane (Figure 11k). An advanced model related to PET was previously configured using extreme machine learning and a sparrow search algorithm (SSA), but it was mainly used to estimate the

evapotranspiration rate and not optimize it [21]. On the other hand, the ASO_{Th}, DE_{Th}, and MVO_{Th} developed here were deployed to determine the optimum temperature and irradiation light period with the corresponding derivative Thornthwaite parameters (Table 2). In general, the optimized Thornthwaite PET models in this study are ranked in descending order of preference based on the resulting optimized PET value: $ASO_{Th} > DE_{Th} > MVO_{Th}$ (Table 2). Hence, it should be noted that the developed evapotranspiration models in this study highlighted the non-linear and interactive processes in evapotranspiration that have a significant impact on both the microscopic and macroscopic features of a fruit-bearing tree like papaya. It is also confirmative that even for smaller regions, PET can be used as an indicator of water-use efficiency. Note that heat index and extended heat index cannot be manually controlled, but they are the extended effects of controlling the temperature of the enclosed environment and the duration of the light period. That means there would be very little water volume that can be evaporated and transpired from the area; hence, available water will be used by the plant optimally. As demonstrated in this study, the designed controlled system, incorporating the findings of ASO_{Th}, provides optimal water resource utilization by minimizing evaporation and transpiration, thereby allowing for the accumulation of water on the soil surface and within plants [14]. In contrast, the uncontrolled condition (without evolutionary computing integration applied to the natural stressors) with a much higher PET value of 0.283 experiences higher water loss due to faster rates of evaporation and transpiration. Consequently, this leads to rapid drying conditions, particularly during midday [14,15]. The plant roots extend just to forage for available water in the lower depth of the soil system to adapt to the limited-resource and constrained environment, which in return also characterizes the thickening of the xylem vessel (Figures 8a and 9f). The chlorophyll concentration in leaves of uncontrolled treatment dropped mainly because stomata play a crucial role in the exchange of carbon dioxide and oxygen during photosynthesis, which in turn induces the chlorophyll *b* to capture light energy within 453nm and 642 nm wavelengths of light [3,5,45]. For sheltered or controlled environment agriculture, an aspect ratio below 100, such as the ASOTh, implies that the plant easily adapts to limited or driven resources and allocates more nutrients into producing leaves and fruits [6,16], which is the case of the papaya plant in the current study. This finding is supported by the collected data on leaf count in which ASOTh has an average of eight leaves per seedling (Figures 8a and 9e). Moreover, the ASO_{Th} plants have faster adaptability to absorb and utilize light energy and maximized ability to absorb even in low light energy conditions [14–16]. This finding is also an indication that the temperature and light period recommended by ASO_{Th} would lead the plants to photodamage and cause oxidative stress [14]. However, this study is limited to studying young papaya plants and performed no characterization in matured papaya trees. Even so, up to the publication of this study, there have been no other studies conducting optimization or modification of the existing PET models. This optimization of the PET model led to a desired enclosed environment design for papaya Sinta F1 growth. This limits the comparison of the study only with uncontrolled environments for cultivation. Furthermore, for the continuation of the study, an observation of changes in trunk diameter, plant height, and fruit quality at later growth stages is a must to compare the results with other studies that optimized their irrigation system based on PET models.

In the view of artificial intelligence, it is mainly deep neural networks and artificial neural networks that have been integrated with the PET model for estimation of water use only [19,22], and these have no specific feedback to the biosystem. Hence, the ASO-based Thornthwaite model developed in the current study serves as proof of the initial improvement of the limitations of the existing model, particularly in terms of potentially inaccurate estimations for regions of high irradiation exposure.
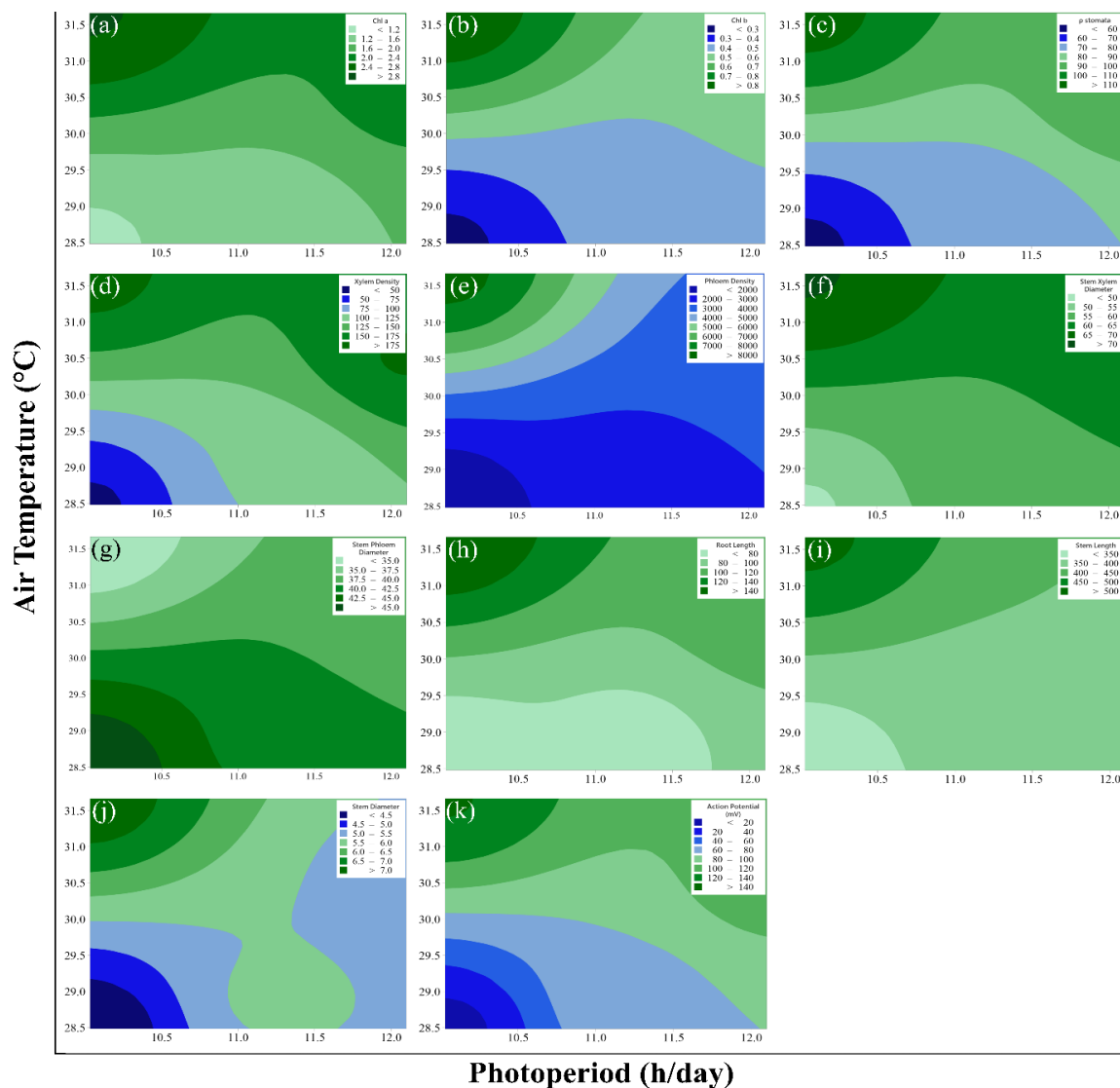
Figure 11. Contour graphs of functional relationships of Thornthwaite PET and crop parameters: (**a**) Chl a, (**b**) Chl b, (**c**) stomata density, (**d**,**e**) root xylem and phloem densities, (**f**,**g**) stem xylem and phloem densities, (**h**,**i**) root and stem lengths, (**j**) stem diameter, and (**k**) action potential from stem membrane, as affected by air temperature and light period.

Unlike default PET models that can be only useful for large geographical cultivation regions and are susceptible to global warming and abrupt changes in environmental pre-growth factors of crops, the developed ASO-based Thornthwaite model is applicable anywhere on Earth if there is a control system that will maintain the in-chamber setting. The consideration of having a controlled environment agriculture setup with a standard PET model in this study is a strategic approach to enhancing food production. Supplying enough information to farmers through installed meteorological sensors will allow data-centered farming capable of providing informed decisions and automated decision management feedback to extendly improve the growth of crops. Furthermore, over- and under-irrigation and negative environmental impacts caused by nutrient leaching will be prevented. Hence, through this study, the Thornthwaite model was optimized and proven applicable for enhancing papaya cultivation.

5. Conclusions

This study has shown that advanced physics-based and evolutionary computing algorithms can be integrated with Thornthwaite potential evapotranspiration (PET) models

to modify and optimize the induced growth of papaya plants, making it site-specific and crop-specific. This mainly solves the limitation of the Thornthwaite PET model which has the potential of inaccurate estimation for regions of high irradiation exposure, indirectly, and the voluminous requirement of having lots of parameter data. Three optimization algorithms were explored and configured in this study, namely, atom search (ASO), differential evolution (DE), and multiverse (MVO) optimizers, to determine the best global combination of configurable Thornthwaite PET for a controlled environment and compared with the uncontrolled treatment of cultivating the papaya Sinta F1 cultivar. Among these four treatments where papaya seedlings were exposed in three replicates in 90 days, the ASO-optimized Thornthwaite PET-treated seedlings resulted in the highest chlorophyll a and b concentrations, densest stomatal density, concentrated root and stem xylem and phloem vessels, considerable root and stem length, most formed leaf count, and strongest action potentials coming from stem membrane for both light periods and dark periods. This is based on temperature and light period values of 31.664 °C and 10.033 h per day, respectively, configurable in a closed environment agriculture for assured vegetative seedling year-round production. The differential impacts of ASO-based Thornthwaite PET make it the most recommended setting for the papaya Sinta F1 cultivar by elucidating its impacts on its vegetative growth parameters. The ASO-based Thornthwaite PET promotes an adjusted and acceptable stem length and thickness ratio, which helps the plant to mechanically support its branching leaves and potential fruits during the fruiting stage. Additionally, there is an enhanced chlorophyll a and b ratio that extends the absorption energy spectrum for plants exhibiting photosynthesis. The adjustment of the Thornthwaite PET could increase crop growth and sustainability in precision farming, while the frequency and volume of demand required for the papaya seedlings may be adjusted in accordance with a reduced, calculated PET. Unlike default PET models that are only useful for large geographical cultivation regions and are susceptible to global warming and abrupt changes in environmental pre-growth factors of crops, the developed ASO-based Thornthwaite is applicable anywhere on Earth as long as there is a control system that will maintain the in-chamber setting. However, the developed ASO_{Th} in this study was only tested for papaya seedlings to young plant stages. Further research should be carried out to characterize the vegetative and fruiting stage of papaya Sinta F1 and other varieties under the same environmental settings by following the ASO-based Thornthwaite PET.

Author Contributions: Conceptualization, R.C.II, J.J.B., A.G.J. and A.B.; methodology, R.C.II, J.J.B., A.G.J. and A.B.; software, R.C.II, J.J.B. and A.G.J.; validation, R.C.II; formal analysis, R.C.II and A.B.; investigation, R.C.II, J.J.B., A.G.J. and A.B.; resources, R.C.II; data curation, R.C.II; writing—original draft preparation, R.C.II, J.J.B. and A.G.J.; writing—review and editing, R.C.II and A.B.; visualization, R.C.II; supervision, R.C.II; project administration, R.C.II; funding acquisition, R.C.II and A.B. All authors have read and agreed to the published version of the manuscript.

Data Availability Statement: The data presented in this study are available on request from the corresponding author. The data are not publicly available due to on-going analysis for another article publication.

Conflicts of Interest: The authors declare no conflict of interest. The funders had no role in the design of the study; in the collection, analyses, or interpretation of data; in the writing of the manuscript; or in the decision to publish the results.

References

1. Strock, C.F.; Burridge, J.D.; Niemiec, M.D.; Brown, K.M.; Lynch, J.P. Root Metaxylem and Architecture Phenotypes Integrate to Regulate Water Use under Drought Stress. *Plant Cell Environ.* **2021**, *44*, 49–67. [CrossRef] [PubMed]
2. Jiménez, V.M.; Mora-Newcomer, E.; Gutiérrez-Soto, M.V. Biology of the Papaya Plant. In *Genetics and Genomics of Papaya*; Springer: New York, NY, USA, 2014; pp. 17–33.
3. de Lima, R.S.N.; de Assis Figueiredo, F.A.M.M.; Martins, A.O.; de Deus, B.C.D.S.; Ferraz, T.M.; de Assis Gomes, M.D.M.; de Sousa, E.F.; Glenn, D.M.; Campostrini, E. Partial Rootzone Drying (PRD) and Regulated Deficit Irrigation (RDI) Effects on Stomatal Conductance, Growth, Photosynthetic Capacity, and Water-Use Efficiency of Papaya. *Sci. Hortic.* **2015**, *183*, 13–22. [CrossRef]
4. Cabrera, J.A.; Ritter, A.; Raya, V.; Pérez, E.; Lobo, M.G. Papaya (*Carica papaya* L.) Phenology under Different Agronomic Conditions in the Subtropics. *Agriculture* **2021**, *11*, 173. [CrossRef]
5. Olubode, O.O.; Odeyemi, O.M.; Aiyelaagbe, I.O.O. Influence of Environmental Factors and Production Practices on the Growth and Productivity of Pawpaw (*Carica papaya* L.) in South Western Nigeria—A Review. *Fruits* **2016**, *71*, 341–361. [CrossRef]
6. Campostrini, E.; Schaffer, B.; Ramalho, J.D.C.; González, J.C.; Rodrigues, W.P.; da Silva, J.R.; Lima, R.S.N. Chapter 19—Environmental Factors Controlling Carbon Assimilation, Growth, and Yield of Papaya (*Carica papaya* L.) Under Water-Scarcity Scenarios. In *Water Scarcity and Sustainable Agriculture in Semiarid Environment*; García Tejero, I.F., Durán Zuazo, V.H., Eds.; Academic Press: Cambridge, MA, USA, 2018; pp. 481–505, ISBN 978-0-12-813164-0.
7. Sharma, V. Impact Climate Change on Crop Water Requirement of Different Orchard Crops for Agro-Climatic Condition of Udaipur, Rajasthan. *Indian J. Ecol.* **2020**, *47*, 12–16.
8. Migliaccio, K.W.; Schaffer, B.; Crane, J.H.; Davies, F.S. Plant Response to Evapotranspiration and Soil Water Sensor Irrigation Scheduling Methods for Papaya Production in South Florida. *Agric. Water Manag.* **2010**, *97*, 1452–1460. [CrossRef]
9. Snyder, R.L.; Marras, S.; Spano, D. Climate Change Impact on Evapotranspiration, Heat Stress and Chill Requirements. *AGU Fall Meet. Abstr.* **2013**, *2013*, GC13B-1068.
10. Nistor, M.-M.; Mîndrescu, M.; Petrea, D.; Nicula, A.-S.; Rai, P.K.; Benzaghta, M.A.; Dezsi, Ş.; Hognogi, G.; Porumb-Ghiurco, C.G. Climate Change Impact on Crop Evapotranspiration in Turkey during the 21st Century. *Meteorol. Appl.* **2019**, *26*, 442–453. [CrossRef]
11. Moretti, C.L.; Mattos, L.M.; Calbo, A.G.; Sargent, S.A. Climate Changes and Potential Impacts on Postharvest Quality of Fruit and Vegetable Crops: A Review. *Food Res. Int.* **2010**, *43*, 1824–1832. [CrossRef]
12. Subedi, S. Climate Change Effects of Nepalese Fruit Production. *MedCrave* **2019**, *9*, 141–145. [CrossRef]
13. Joshi, V.P.; Chauhan, P.M. Combating Climate Change through Off-Seasonally Raising Seedling of Papaya (*Carica papaya* L.) in Protected Environment. *Res. Crop.* **2016**, *17*, 298. [CrossRef]
14. Carvalho, E.V.; Cifuentes-Arenas, J.C.; Raiol-Junior, L.L.; Stuchi, E.S.; Girardi, E.A.; Lopes, S.A. Modeling Seasonal Flushing and Shoot Growth on Different Citrus Scion-Rootstock Combinations. *Sci. Hortic.* **2021**, *288*, 110358. [CrossRef]
15. Orlandi, F.; Bonofiglio, T.; Romano, B.; Fornaciari, M. Qualitative and Quantitative Aspects of Olive Production in Relation to Climate in Southern Italy. *Sci. Hortic.* **2012**, *138*, 151–158. [CrossRef]
16. Mobe, N.T.; Dzikiti, S.; Dube, T.; Mazvimavi, D.; Ntshidi, Z. Modelling Water Utilization Patterns in Apple Orchards with Varying Canopy Sizes and Different Growth Stages in Semi-Arid Environments. *Sci. Hortic.* **2021**, *283*, 110051. [CrossRef]
17. Kumar, S.; Dey, P. Effects of Different Mulches and Irrigation Methods on Root Growth, Nutrient Uptake, Water-Use Efficiency and Yield of Strawberry. *Sci. Hortic.* **2011**, *127*, 318–324. [CrossRef]
18. Ghaderi, A.; Dasineh, M.; Shokri, M.; Abraham, J. Estimation of Actual Evapotranspiration Using the Remote Sensing Method and SEBAL Algorithm: A Case Study in Ein Khosh Plain, Iran. *Hydrology* **2020**, *7*, 36. [CrossRef]
19. Elbeltagi, A.; Deng, J.; Wang, K.; Malik, A.; Maroufpoor, S. Modeling Long-Term Dynamics of Crop Evapotranspiration Using Deep Learning in a Semi-Arid Environment. *Agric. Water Manag.* **2020**, *241*, 106334. [CrossRef]
20. Chia, M.Y.; Huang, Y.F.; Koo, C.H. Swarm-Based Optimization as Stochastic Training Strategy for Estimation of Reference Evapotranspiration Using Extreme Learning Machine. *Agric. Water Manag.* **2021**, *243*, 106447. [CrossRef]
21. Jia, Y.; Su, Y.; Zhang, R.; Zhang, Z.; Lu, Y.; Shi, D.; Xu, C.; Huang, D. Optimization of an Extreme Learning Machine Model with the Sparrow Search Algorithm to Estimate Spring Maize Evapotranspiration with Film Mulching in the semiarid Regions of China. *Comput. Electron. Agric.* **2022**, *201*, 107298. [CrossRef]
22. Pandorfi, H.; Bezerra, A.C.; Atarassi, R.T.; Vieira, F.M.C.; Barbosa Filho, J.A.D.; Guiselini, C. Artificial Neural Networks Employment in the Prediction of Evapotranspiration of Greenhouse-Grown Sweet Pepper. *Rev. Bras. Eng. Agríc. Ambient.* **2016**, *20*, 507–512. [CrossRef]
23. Zhu, B.; Feng, Y.; Gong, D.; Jiang, S.; Zhao, L.; Cui, N. Hybrid Particle Swarm Optimization with Extreme Learning Machine for Daily Reference Evapotranspiration Prediction from Limited Climatic Data. *Comput. Electron. Agric.* **2020**, *173*, 105430. [CrossRef]
24. Wu, L.; Zhou, H.; Ma, X.; Fan, J.; Zhang, F. Daily Reference Evapotranspiration Prediction Based on Hybridized Extreme Learning Machine Model with Bio-Inspired Optimization Algorithms: Application in Contrasting Climates of China. *J. Hydrol.* **2019**, *577*, 123960. [CrossRef]
25. Gao, L.; Gong, D.; Cui, N.; Lv, M.; Feng, Y. Evaluation of Bio-Inspired Optimization Algorithms Hybrid with Artificial Neural Network for Reference Crop Evapotranspiration Estimation. *Comput. Electron. Agric.* **2021**, *190*, 106466. [CrossRef]

26. Hernández-Salazar, J.A.; Hernández-Rodríguez, D.; Hernández-Cruz, R.A.; Ramos-Fernández, J.C.; Márquez-Vera, M.A.; Trejo-Macotela, F.R. Estimation of the Evapotranspiration Using ANFIS Algorithm for Agricultural Production in Greenhouse. In Proceedings of the 2019 IEEE International Conference on Applied Science and Advanced Technology (iCASAT), Queretaro, Mexico, 27–28 November 2019; pp. 1–5.

27. Shamshiri, R.R.; Kalantari, F.; Ting, K.C.; Thorp, K.R.; Hameed, I.A.; Weltzien, C.; Ahmad, D.; Shad, Z.M. Advances in Greenhouse Automation and Controlled Environment Agriculture: A Transition to Plant Factories and Urban Agriculture. *Int. J. Agric. Biol. Eng.* **2018**, *11*, 1–22. [CrossRef]

28. Arcel, M.M.; Lin, X.; Huang, J.; Wu, J.; Zheng, S. The Application of LED Illumination and Intelligent Control in Plant Factory, a New Direction for Modern Agriculture: A Review. *J. Phys. Conf. Ser.* **2021**, *1732*, 012178. [CrossRef]

29. Siropyan, M.; Celikel, O.; Pinarer, O. Artificial Intelligence Driven Vertical Farming Management System. In *Lecture Notes in Engineering and Computer Science: Proceedings of The World Congress on Engineering and Computer Science, San Francisco, CA, USA, 19–21 October 2016*; Ao, S.I., Douglas, C., Grundfest, W.S., Eds.; Newswood Limited: San Francisco, CA, USA, 2016.

30. Hemming, S.; de Zwart, F.; Elings, A.; Righini, I.; Petropoulou, A. Remote Control of Greenhouse Vegetable Production with Artificial Intelligence—Greenhouse Climate, Irrigation, and Crop Production. *Sensors* **2019**, *19*, 1807. [CrossRef] [PubMed]

31. Kasatkin, V.; Kasatkina, N.; Svalova, M. *Intelligent Process Control System of Water Treatment for Nutrient Solutions of Drip Irrigation*; Atlantis Press: Paris, France, 2019; pp. 289–292.

32. Roy, D.K.; Lal, A.; Sarker, K.K.; Saha, K.K.; Datta, B. Optimization Algorithms as Training Approaches for Prediction of Reference Evapotranspiration Using Adaptive Neuro Fuzzy Inference System. *Agric. Water Manag.* **2021**, *255*, 107003. [CrossRef]

33. Hekimoğlu, B. Optimal Tuning of Fractional Order PID Controller for DC Motor Speed Control via Chaotic Atom Search Optimization Algorithm. *IEEE Access* **2019**, *7*, 38100–38114. [CrossRef]

34. Hao, Z.-F.; Guo, G.-H.; Huang, H. A Particle Swarm Optimization Algorithm with Differential Evolution. In Proceedings of the 2007 International Conference on Machine Learning and Cybernetics, Hong Kong, China, 19–22 August 2007; Volume 2, pp. 1031–1035.

35. Rosales Muñoz, A.A.; Grisales-Noreña, L.F.; Montano, J.; Montoya, O.D.; Perea-Moreno, A.-J. Application of the Multiverse Optimization Method to Solve the Optimal Power Flow Problem in Alternating Current Networks. *Electronics* **2022**, *11*, 1287. [CrossRef]

36. Gharehbaghi, A.; Kaya, B. Calibration and Evaluation of Six Popular Evapotranspiration Formula Based on the Penman-Monteith Model for Continental Climate in Turkey. *Phys. Chem. Earth Parts A/B/C* **2022**, *127*, 103190. [CrossRef]

37. Wu, Z.; Cui, N.; Zhao, L.; Han, L.; Hu, X.; Cai, H.; Gong, D.; Xing, L.; Chen, X.; Zhu, B.; et al. Estimation of Maize Evapotranspiration in Semi-Humid Regions of Northern China Using Penman-Monteith Model and Segmentally Optimized Jarvis Model. *J. Hydrol.* **2022**, *607*, 127483. [CrossRef]

38. de Guia, J.D.; Concepcion, R.S.; Calinao, H.A.; Alejandrino, J.; Dadios, E.P.; Sybingco, E. Using Stacked Long Short Term Memory with Principal Component Analysis for Short Term Prediction of Solar Irradiance Based on Weather Patterns. In Proceedings of the 2020 IEEE Region 10 Conference (Tencon), Osaka, Japan, 16–19 November 2020; pp. 946–951.

39. de Guia, J.D.; Concepcion, R.S., II; Calinao, H.A.; Tobias, R.R.; Dadios, E.P.; Bandala, A.A. Solar Irradiance Prediction Based on Weather Patterns Using Bagging-Based Ensemble Learners with Principal Component Analysis. In Proceedings of the 2020 IEEE 8th R10 Humanitarian Technology Conference (R10-HTC), Kuching, Malaysia, 1–3 December 2020; pp. 1–6.

40. Concepcion, R.; Alejandrino, J.; Mendigoria, C.H.; Dadios, E.; Bandala, A.; Sybingco, E.; Vicerra, R.R. Lactuca Sativa Leaf Extract Concentration Optimization Using Evolutionary Strategy as Photosensitizer for TiO$_2$-Filmed Grätzel Cell. *Optik* **2021**, *242*, 166931. [CrossRef]

41. Zhao, W.; Wang, L.; Zhang, Z. A Novel Atom Search Optimization for Dispersion Coefficient Estimation in Groundwater. *Future Gener. Comput. Syst.* **2019**, *91*, 601–610. [CrossRef]

42. Zhang, H.; Liu, T.; Ye, X.; Heidari, A.A.; Liang, G.; Chen, H.; Pan, Z. Differential Evolution-Assisted Salp Swarm Algorithm with Chaotic Structure for Real-World Problems. *Eng. Comput.* **2023**, *39*, 1735–1769. [CrossRef]

43. Lynn, N.; Ali, M.Z.; Suganthan, P.N. Population Topologies for Particle Swarm Optimization and Differential Evolution. *Swarm Evol. Comput.* **2018**, *39*, 24–35. [CrossRef]

44. Kumar, M.B.H.; Balasubramaniyan, S.; Padmanaban, S.; Holm-Nielsen, J.B. Wind Energy Potential Assessment by Weibull Parameter Estimation Using Multiverse Optimization Method: A Case Study of Tirumala Region in India. *Energies* **2019**, *12*, 2158. [CrossRef]

45. Concepcion, R.; Lauguico, S.; Alejandrino, J.; Dadios, E.; Sybingco, E.; Bandala, A. Aquaphotomics Determination of Nutrient Biomarker for Spectrophotometric Parameterization of Crop Growth Primary Macronutrients Using Genetic Programming. *Inf. Process. Agric.* **2022**, *9*, 497–513. [CrossRef]

46. Concepcion, R., II; Dadios, E.; Bandala, A.; Cuello, J.; Kodama, Y. Hybrid Genetic Programming and Multiverse-Based Optimization of Pre-Harvest Growth Factors of Aquaponic Lettuce Based on Chlorophyll Concentration. *Int. J. Adv. Sci. Eng. Inf. Technol.* **2021**, *11*, 2128. [CrossRef]